

ChemComm

Accepted Manuscript



This is an *Accepted Manuscript*, which has been through the Royal Society of Chemistry peer review process and has been accepted for publication.

Accepted Manuscripts are published online shortly after acceptance, before technical editing, formatting and proof reading. Using this free service, authors can make their results available to the community, in citable form, before we publish the edited article. We will replace this *Accepted Manuscript* with the edited and formatted *Advance Article* as soon as it is available.

You can find more information about *Accepted Manuscripts* in the [Information for Authors](#).

Please note that technical editing may introduce minor changes to the text and/or graphics, which may alter content. The journal's standard [Terms & Conditions](#) and the [Ethical guidelines](#) still apply. In no event shall the Royal Society of Chemistry be held responsible for any errors or omissions in this *Accepted Manuscript* or any consequences arising from the use of any information it contains.

Cite this: DOI: 10.1039/coxx00000x

www.rsc.org/xxxxxx

ARTICLE TYPE

A sensitive electrochemical aptasensor based on the co-catalysis of hemin/G-quadruplex, platinum nanoparticles and flower-like MnO₂ nanospheres functionalized multi-walled carbon nanotubes

Wenju Xu*, Shuyan Xue, Huayu Yi, Pei Jing, Yaqin Chai, Ruo Yuan*

Received (in XXX, XXX) Xth XXXXXXXXX 20XX, Accepted Xth XXXXXXXXX 20XX

DOI: 10.1039/b000000x

In this work, a sensitive electrochemical aptasensor for the detection of thrombin (TB) is developed and demonstrated based on the co-catalysis of hemin/G-quadruplex, platinum nanoparticles (PtNPs) and flower-like MnO₂ nanospheres functionalized multi-walled carbon nanotubes (MWCNTs-MnO₂).

Quantitative detection of thrombin (TB) is of great importance in clinical research and diagnosis owing to the central role of TB in anti-clotting therapeutics, cardiovascular diseases, and various proinflammatory activities.¹ Recently, aptamer-based sensors (aptasensors) including fluorescent aptasensors,² electrochemical aptasensors,³ colorimetric aptasensors⁴ and surface plasmon resonance aptasensors⁵ have been developed for TB detection. Among them, electrochemical aptasensors show significant predominance including portability, simple operation, fast response time and inherent miniaturization.⁶ Thus, it is fascinating to use electrochemical aptasensors for protein detection.⁷ In order to improve the sensitivity of detection method, various signal amplification strategies have been developed, such as rolling circle amplification,⁸ enzyme labeling amplification⁹ and polymerase chain reaction.¹⁰ Among these strategies, enzyme labeling amplification has been widely used during the past few decades because of the high selectivity and sensitivity.¹¹ However, the practical applications of such enzyme-based strategy are limited due to complicated immobilization procedures, environmental instability and high cost.¹²

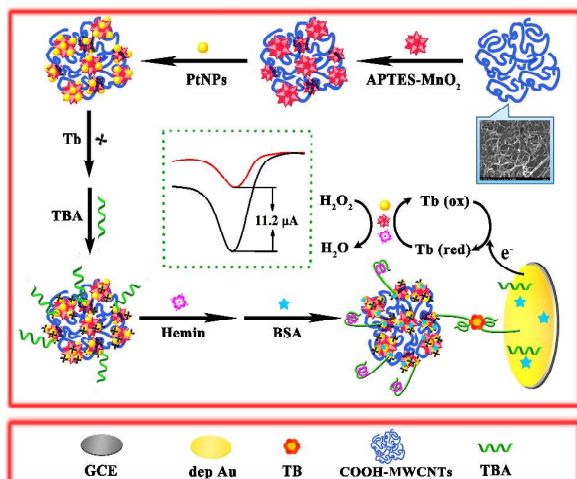
To overcome these limitations, various metal and metal oxide nanomaterials have been explored as alternative electrochemical catalysts to fabricate enzyme-free and sensitive electrochemical aptasensors.¹³ As a kind of metal oxide nanomaterials, flower-like manganese oxide (MnO₂) nanospheres possess desirable properties such as good chemical stability, high catalytic activity, low cost and environmental friendliness.¹⁴ Particularly, flower-like MnO₂ nanospheres show the peroxidase-like activity,¹⁵ providing promising opportunities for the development of signal amplification strategy. In addition, flower-like nanostructures of MnO₂ can provide a large specific surface area, potentially making them excellent candidate for capturing numerous biomolecules. So, flower-like MnO₂ nanospheres should be extremely attractive in the area of biosensors. However, only

few works to date involving in electrochemiluminescent immunosensors^{15b} and fluorescent biosensors¹⁶ were reported. Especially, electrochemical aptasensors based on flower-like MnO₂ has been received little attention. Moreover, multi-walled carbon nanotubes (MWCNTs) with good conductivity, low electrical resistance, outstanding charge-transport ability and high accessible surface area,¹⁷ has been widely employed in various biosensors. Therefore, the combination of flower-like MnO₂ nanospheres and MWCNTs may further expand the possibility of utilization of the nanocomposite (MWCNTs-MnO₂) as a promising nanocarrier for fabricating sensitive electrochemical biosensors.

Herein, we proposed an enzyme-free electrochemical aptasensor for TB detection based on flower-like MnO₂ nanospheres functionalized MWCNTs as a nanocarrier. Firstly, flower-like MnO₂ nanospheres were synthesized by a simple chemistry route, then functionalized with APTES, and finally attached to MWCNTs to form MWCNTs-MnO₂ (see ESI† for details). The resulting nanocomposite can provide a large surface area, excellent electrocatalytic activity and high stability, which would improve immobilization sites for biological molecules, allow remarkable amplification of electrochemical signal and contribute to an improved sensitivity. Secondly, large amounts of platinum nanoparticles (PtNPs), redox-active Tb and hemin/G-quadruplex horseradish peroxidase-mimicking DNAzyme¹⁸ could be immobilized on MWCNTs-MnO₂ nanocomposite, which further enhanced the electrochemical signal. Flower-like MnO₂ nanospheres and MWCNTs-MnO₂ nanocomposite were characterized by scanning electron microscope (SEM) and X-ray photoelectron spectroscopy (XPS) (see ESI† for details).

The protocol of the proposed TB aptasensor was achieved by using a triple amplified strategy. As shown in Scheme 1, MWCNTs-MnO₂ nanocomposite was firstly obtained through attachment of flower-like MnO₂ nanospheres onto the surface of MWCNTs. And then, it was successively conjugated using large amounts of PtNPs, redox-active Tb, hemin/G-quadruplex and blocking agent bovine serum albumin (BSA), resulting in the final formation of secondary aptamer (hemin/G-quadruplex conjugated MWCNTs-MnO₂-PtNPs-Tb). Through “sandwich” tactics, the secondary aptamer was captured onto the electrode surface modified with AuNPs,

TBA and target TB, indicating the formation of the proposed apt sensor (see ESI† for details). Finally, an obvious amplified electrochemical signal can be successfully observed due to the co-catalysis of flower-like MnO₂ nanospheres, PtNPs and hemin/G-quadruplex to the reduction of H₂O₂ added in electrolytic cell. The strategy of the signal amplification was designed as follows: (i) Flower-like MnO₂ nanospheres with large surface area exhibit high catalytic activity toward H₂O₂ reduction, leading to the effective signal amplification; (ii) Large amounts of immobilized PtNPs with excellent electrocatalytic activity can further enhance electrochemical signal; (iii) Hemin/G-quadruplex exhibits horseradish peroxidase-mimicking DNAzyme, allowing significant signal amplification in the presence of H₂O₂. Moreover, the amplification of current response of different secondary aptamer bioconjugates was compared (see ESI† for details). So such the co-catalysis can greatly promote electron transfer of redox-active Tb and efficiently improve sensitivity of the proposed TB electrochemical aptasensor.



Scheme 1. Schematic diagram for the fabrication of the electrochemical aptasensor and signal amplification strategy.

In order to monitor and characterize the modified electrode during the stepwise fabrication, CV experiments in 5 mM K₃[Fe(CN)₆]/K₄[Fe(CN)₆] were conducted and the results are shown in Fig. 1. As we can see, the bare GCE exhibited a typical pair of reversible redox peak which was corresponding to the reversible redox reaction (curve a). In the presence of electrodeposited AuNPs, the resulting electrode showed increased redox current (curve b), owing to the high conductivity of AuNPs for promotion of electron transfer. When NH₂-TBA was modified on the electrode, a decreased current was observed (curve c), indicating that NH₂-TBA hindered the electron transfer tunnel. A decreased peak current (curve d) was also obtained upon the immobilization of non-conductive BSA on the modified electrode. In addition, the peak current further decreased with the incubation of 10 nM TB, suggesting the formation of aptamer-TB complex which obstructed the tunnel of electron shuttle.

In this work, experimental conditions were optimized (see ESI† for details). Under optimal conditions, the proposed electrochemical aptasensor was applied for the quantitative detection of TB at different concentrations. The analytical

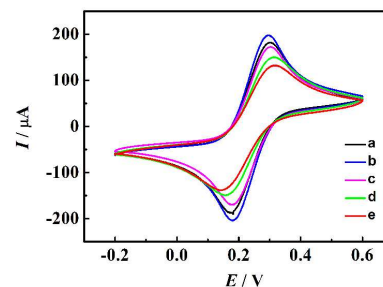


Fig. 1 CVs of modification process of the electrode in 5 mM K₃[Fe(CN)₆]/K₄[Fe(CN)₆] with 100 mV/s scan rate: (a) GCE, (b) AuNPs/GCE, (c) NH₂-TBA/AuNPs/GCE, (d) BSA/ NH₂-TBA/AuNPs/GCE, (e) TB/BSA/NH₂-TBA/AuNPs/ GCE. 2.5 μM NH₂-TBA and 40 min TB incubation time.

performance was assessed by DPV in 0.1 M PBS containing 3.68 mM H₂O₂, and the results are shown in Fig. 2. From Fig. 2A, we can see the current response was enhanced gradually with the increasing concentrations of TB. As seen from Fig. 2B, the calibration plots exhibited a good linear relationship between the electrochemical signal and the logarithm of the analyte concentrations, suggesting the successful immobilization of more secondary aptamer as well as the redox mediator Tb on the electrode surface. For TB (Fig. 2B), the corresponding regression equation was $I (\mu\text{A}) = -2.305 \lg c_{\text{TB}} (\text{nM}) - 18.42$ in the range from 1 pM to 30 nM with correlation coefficient of 0.9954. Based on literature method,¹⁹ the detection limit of the proposed aptasensor (defined as $DL=3S_B/m$, where S_B is the standard deviation of the blank and m is the slope of the corresponding calibration curve) was 0.040 pM. Compared with other TB detection approaches obtained from published studies, the proposed signal amplification strategy could give more remarkable sensitivity and lower detection limit (See ESI† Table S1 and S2). This should attribute to the corporate catalysis of abundant immobilized flower-like MnO₂ nanospheres, PtNPs and hemin/G-quadruplex toward H₂O₂ reduction.

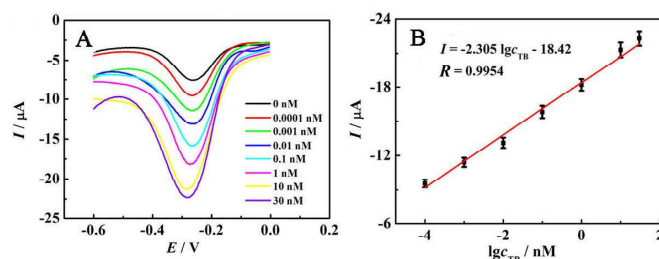


Fig. 2 (A) DPV responses of the proposed aptasensor to different concentrations of TB in 0.1 M PBS (pH 7.0) with 3.68 mM H₂O₂ and (B) the resultant linear calibration curve for TB. Measurements were carried out with 50 mV amplitude of and 0.05 s pulse width. Error bars: SD, $n=3$.

The specificity of a sensor is a very important characteristic in analyzing biological samples. DPV response of such interfering substances as hemoglobin (Hb), bovine serum albumin (BSA) and human IgG were measured in this study. As can be seen in Fig. 3, the proposed aptasensor showed dramatic increased current signal toward target TB (10 nM), whereas the current response were negligible in the

detection of Hb (100 nM), BSA (100 nM) and human IgG (100 nM). Moreover, a similar dramatic increase could be observed in the presence of a mixture of 10 nM TB and the interfering substances. These results revealed the high specific affinity of the fabricated aptasensor to TB.

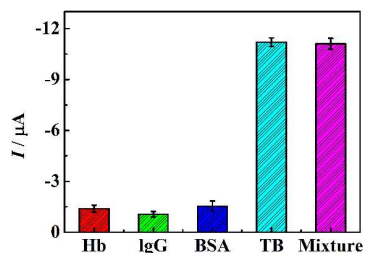


Fig. 3 The specificity of the electrochemical aptasensor for the target TB (10 nM) compared with other interfering substances: Hb (100 nM), IgG (100 nM), BSA (100 nM) and their mixture with 10 nM TB. Error bars: SD, $n=3$. Other conditions as shown in Fig. 2.

To evaluate the reproducibility of the aptasensor, four aptasensors were prepared under same conditions for the repeated measurements of TB (10 nM). Reproducible electrochemical signal for the four aptasensors and relative standard deviation (RSD) of 5.6% were obtained, suggesting the satisfactory reproducibility of the proposed aptasensor. In addition, the stability of the aptasensor was investigated by detecting the electrochemical signal after 10 days of storage at 4 °C. The CV peak current could retain 91.7% of its initial response for 10 nM TB, demonstrating that the proposed aptasensor possessed acceptable stability.

To investigate the reliability and practical applicability of the aptasensor, different amounts of target TB were added into the 10-fold-diluted human serum samples (obtained from Xinqiao Hospital of Chongqing, China) and DPV signals of the obtained samples were subsequently recorded. Seen from ESI† Table S3, acceptable results with recoveries ranging from 97.5% to 109% and RSDs from 4.6% to 7.1% for TB detection were achieved, thereby clearly revealing a satisfactory reliability of our protocol.

In conclusion, we have successfully designed a sensitive enzyme-free electrochemical aptasensor for TB detection based on a triple signal amplification strategy resulting from hemin/G-quadruplex conjugated MWCNTs-MnO₂-PtNPs-Tb. The employment of MWCNTs-MnO₂ nanocomposite as an ideal nanocarrier led to attachment of large amounts of PtNPs hemin/G-quadruplex and redox-active Tb on the electrode surface, paving the way for the amplified electrochemical detection. Furthermore, the co-electrocatalytic behavior of flower-like MnO₂ nanospheres, PtNPs and hemin/G-quadruplex toward H₂O₂ reduction greatly amplified electrochemical signal, achieving high sensitivity of the aptasensor. Compared with other published methods, the proposed aptasensor exhibited improved electrochemical characteristics, providing an efficient and simple strategy for protein diagnostics in clinical application.

This research has been carried out with financial support from Natural Science Foundation of Chongqing City (CSTC-2011BA7003, CSTC-2010BB4121), NNSF of China

(21075100, 21105081, 21275119), Ministry of Education of China (Project 708073) and the Fundamental Research Funds for the Central Universities (XDJK2013A008, 2013A027).

Notes and references

Shuyan Xue is the same role as the first author in contribution to this paper.

Key Laboratory of Luminescent and Real-Time Analytical Chemistry (Southwest University), Ministry of Education, School of Chemistry and Chemical Engineering, Southwest University, Chongqing 400715, PR China

Fax: +86-23-68253172; Tel: +86-23-68252277

E-mail: xwju@swu.edu.cn (W.J. Xu); yuanruo@swu.edu.cn (R. Yuan).

† Electronic Supplementary Information (ESI) available: [details of any supplementary information available should be included here]. See DOI:10.1039/b000000x/

- a) F. Y. Yeh, T. Y. Liu, I. H. Tseng, C. W. Yang, L. C. Lu and C. S. Lin, *Biosens. Bioelectron.*, 2014, **61**, 336–343; b) W. J. Xu, H. Y. Yi, Y. L. Yuan, P. Jing, Y. Q. Chai, R. Yuan and G. S. Wilson, *Biosens. Bioelectron.*, 2015, **64**, 423–428.
- M. Oishi, S. Nakao and D. Kato, *Chem. Commun.*, 2014, **50**, 991–993.
- D. P. Tang, J. Tang, Q. F. Li, B. L. Su and G. N. Chen, *Anal. Chem.*, 2011, **83**, 7255–7259.
- B. F. Ye, Y. J. Zhao, Y. Cheng, T. T. Li, Z. Y. Xie, X. W. Zhao and Z. Z. Gu, *Nanoscale*, 2012, **4**, 5998–6003.
- L. Wang, C. Z. Zhu, L. Han, L. H. Jin, M. Zhou and S. J. Dong, *Chem. Commun.*, 2011, **47**, 7794–7796.
- a) B. Q. Liu, Y. L. Cui, D. P. Tang, H. H. Yang and G. N. Chen, *Chem. Commun.*, 2012, **48**, 2624–2626; b) J. Zhao, Y. Y. Zhang, H. T. Li, Y. Q. Wen, X. Y. Fan, F. B. Lin, L. Tan and S. Z. Yao, *Biosens. Bioelectron.*, 2011, **26**, 2297–2303.
- W. Song, H. Li, H. Liang, W. B. Qiang and D. K. Xu, *Anal. Chem.*, 2014, **86**, 2775–2783.
- S. Bi, L. Li and S. S. Zhang, *Anal. Chem.*, **82**, 9447–9454.
- A. X. Zheng, J. R. Wang, J. Li, X. R. Song, G. N. Chen and H. H. Yang, *Chem. Commun.*, 2012, **48**, 374–376.
- M. Yuce, H. Kurt, V. R. S. S. Mokkaipati and H. Budak, *RSC Adv.*, 2014, **4**, 36800–36814.
- X. H. Kang, Z. B. Mai, X. Y. Zou, P. X. Cai and J. Y. Mo, *Anal. Biochem.*, 2007, **363**, 143–150.
- J. Bai and X. Jiang, *Anal. Chem.*, 2013, **85**, 8095–8101.
- a) H. Wei and E. Wang, *Chem. Soc. Rev.*, 2013, **42**, 6060–6093; b) X. L. He, L. F. Tan, D. Chen, X. L. Wu, X. L. Ren, Y. Q. Zhang, X. W. Meng and F. Q. Tang, *Chem. Commun.*, 2013, **49**, 4643–4645; c) C. Zheng, A. X. Zheng, B. Liu, X. L. Zhang, Y. He, J. Li, H. H. Yang and G. N. Chen, *Chem. Commun.*, 2014, **50**, 13103–13106.
- a) J. L. Kang, A. Hirata, L. J. Kang, X. M. Zhang, Y. Hou, L. Y. Chen, C. Li, T. Fujita, K. Akagi and M. W. Chen, *Angew. Chem. Int. Ed.*, 2013, **52**, 1664–1667; b) M. Yoshimoto, C. Iida, A. Kariya, N. Takaki and M. Nakayama, *Electroanalysis*, 2010, **22**, 653–659.
- a) X. Liu, Q. Wang, H. H. Zhao, L. C. Zhang, Y. Y. Su and L. Lv, *Analyst*, 2012, **137**, 4552–4558; b) Y. Zhang, M. Su, L. Ge, S. G. Ge, G. H. Yu and X. R. Song, *Carbon*, 2013, **57**, 22–33; c) F. Y. Cheng, Y. Su, J. Liang, Z. L. Tao and J. Chen, *Chem. Mater.*, 2010, **22**, 898–905.
- D. G. He, X. X. He, K. M. Wang, X. Yang, X. X. Yang, X. C. Li and Z. Zou, *Chem. Commun.*, 2014, **50**, 11049–11052.
- a) J. M. You, Y. N. Jeong, M. S. Ahmed S. K. Kim, Y. C. Choi and S. Jeon, *Biosens. Bioelectron.*, 2011, **26**, 2287–2291; b) M. Cargnello, M. Grzelczak, B. R. González, Z. Syrgiannis, K. Bakhmutsky, V. L. Parola, L. M. L. Marzán, R. J. Gorte, M. Prato and P. Fornasiero, *J. Am. Chem. Soc.*, 2012, **134**, 11760–11766.
- Y. L. Yuan, R. Yuan, Y. Q. Chai, Y. Zhuo, X. Y. Ye, X. X. Gan and L. J. Bai, *Chem. Commun.*, 2012, **48**, 4621–4623.
- A. E. Radi, J. L. A. Sánchez, E. Baldrich and C. K. O’Sullivan, *J. Am. Chem. Soc.*, 2006, **128**, 117–124.